



Research article

UDC 69.04

DOI: 10.34910/MCE.112.6



The shear behavior of anchored groove RC beams

R. Al-Rousan  

Jordan University of Science and Technology, Irbid, Jordan

 rzalrousan@just.edu.jo

Keywords: reinforced concrete, anchored, shear strength, fiber reinforced polymer, experimental

Abstract. The purpose of this research is to find an effectual technique to anchor reinforced concrete (RC) beams that are strengthened with fiber-reinforced polymers (FRP) composites. Eighteen reinforced-with-CFRP beams were designed. The specimens were split into three groups consisting of: 1) eight externally-reinforced-by-CFRP beams, with no anchoring grooves; 2) eight beams similar to the first group, but with anchoring grooves; 3) and control beams, which were left without anchoring. In order to explore their behavior, all of the beam specimens underwent a four-point bending, and were compared to the control beams. The study's focus was on exploring the relationship between the specimens' modes of failure and their displacements due to the applied loads. The obtained results showed that the anchoring technique had a great effectiveness; whereas, the specimens with CFRP and anchor encountered a failure in the form of a separation in the concrete cover, unlike the un-anchored ones, which failed due to premature de-bonding. The study showed that the anchoring grooves had changed the mode of failure to a safer one. The anchoring technique enhanced the capacity of carrying the load, and reduced, to different extents, the mid-span deflection. In addition, the study found that reinforcing the beams by CFRP composites had enhanced the shear capacity of the area of anchorage, leading to an enhancement in the systematic efficiency of anchoring. Overall, the study concluded that the performance of the specimens was highly improved by utilizing the CFRP composite combined with anchored grooves. For much improved RC structural designs, it is of utmost importance to further develop the anchored groove technique to prevent, rather than delay, unpredictable de-bonding of CFRP.

Funding: The author gratefully acknowledges the financial support from Deanship of Scientific Research at Jordan University of Science and Technology under Grant number 2019/507.

Citation: Al-Rousan, R. The shear behavior of anchored groove RC beams. Magazine of Civil Engineering. 2022. 112(4). Article No. 11206. DOI: 10.34910/MCE.112.6

1. Introduction

As it is well-known, the externally-bonded fiber reinforced polymer (FRP) materials are used to repair concrete elements, and enhance their shear and flexure capacities. The beams have been subjected, frequently, to failure in de-bonding, prematurely. Therefore, there has to be a way to strengthen the FRP-concrete bond to delay, or even prevent, the de-bonding issue. The mechanical anchorage technique has been introduced to solve the threat of ill-timed de-bonding, and further strengthen the plain FRP reinforcements. The anchorage technique, although proven to be efficient, still suffers the lack of knowledge and experience among the designers and engineers. Therefore, the anchorage method needs to be further researched, experimentally and numerically, to be more familiar with it, and expand its usages.

A number of researchers reported that it had been so common for the beams, strengthened by externally-bonded FRP, to encounter an ill-time de-bonding failure mode in the FRP-concrete bond. This type of failure has constrained the usages of the FRP reinforcements [1–9]. The FRP external strengthening are most commonly known to be exposed to fail due to the peeling at the end of the FRP plate and mid-span de-bonding. The plate peeling mode of failure results from the shear stresses' conveyance from the

reinforcement material to concrete. As a result, a concrete layer is detached from the reinforcing FRP material, leaving an amount of hanging concrete ranging from few millimeters to the entire concrete cover. It is worth mentioning that the discontinuity of the beam's sectional geometry, at the end of the plate, is the main cause of the shear stresses. This failure mode is brittle; and it has been noticed to take place, mostly, in the beams that are equipped with short plates [10]. As for the mid-span de-bonding, it is created by two causes: the conveyance of shear stresses to the concrete from the plate of FRP; and it begins to emerge of flexure crack close to the area of the load concentration, in the zone of the extreme bending capacity. The generation of the shear stresses is due to the inclination of the plate strain, consequential from deviations in the moment diagram contiguous to the steel reinforcement yielding in tension side and the concentrated load. The mid-span de-bonding failure mode is ductile, unlike the other type. The reason of this is that the beam's behavior is improved in terms of tensile steel yielding, which permits higher deflections [11].

Anchoring the externally-bonded FRP materials, in RC elements, is vital for the optimization of fiber utilization before de-bonding, prematurely. Several researches have been conducted to explore the effectiveness of the anchorage devices in the strengthening of FRP [12–14], and the mechanical anchorage systems [15–23]. The previous studies introduced four methods of anchoring: (i) fasteners of metallic [32–33]; (ii) anchored FRP [25–26]; (iii) FRP composites [27]; (iv) metal plates with nails [28], (v) anchored steel bolted plate [29]; and (vi) Continuous Reinforcement Embedded at Ends (CREatE) [30].

Anchorage systems have shown a great success in delaying, or even avoiding, the de-bonding failure, converting this type of failure, which is brittle, to a less serious one. As a result, it enhances the efficiency of the method of reinforcement using FRP.

This study has been conducted aiming to find an effective, reliable mechanical anchorage technique to strengthen the FRP-reinforced beams. Based on the analysis of the previous researches conducted in this regard, a novel mechanical anchorage method has been introduced, in this work, to treat the de-bonding issue. For the purposes of this study, the structural behavior has been evaluated, experimentally, study on: 8 un-anchored beams strengthened with externally-bonded CFRP; another 8 beams that are strengthened with a combination of externally-bonded CFRP and anchoring grooves; while, lastly, 2 beams were left unanchored, as control beams.

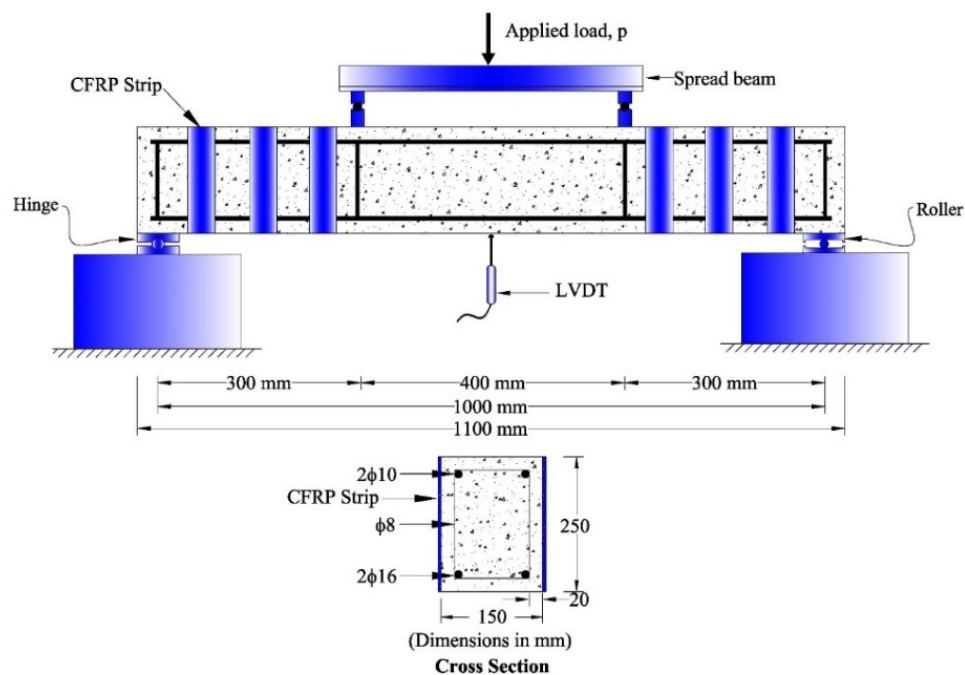


Figure 1. Setup and reinforcement details of the beams.

Table 1. The details of failure of tested shear beams.

Specimen	CFRP Configuration	P_u , kN	Δ_u , mm	ε_f , $\mu\varepsilon$	ε_{CFRP}
SB0	RC beams was unanchored and left as a control	55.7	4.7	---	---
SB1-1S	RC beams external strengthened with 1 Strip of FRP without anchored groove technique	68.4	5.3	5132	$0.31\varepsilon_{fu}$
SB1-2S	RC beams external strengthened with 2 Strips of FRP without anchored groove technique	81.1	5.6	5416	$0.32\varepsilon_{fu}$
SB1-3S	RC beams external strengthened with 3 Strips of FRP without anchored groove technique	95.0	6.0	5727	$0.34\varepsilon_{fu}$
SB1-4S	RC beams external strengthened with 4 Strips of FRP without anchored groove technique	108.5	6.2	5986	$0.36\varepsilon_{fu}$
SB2-1S-G	RC beams external strengthened with 1 Strip of FRP with anchored groove technique	88.0	5.8	6361	$0.38\varepsilon_{fu}$
SB2-2S-G	RC beams external strengthened with 2 Strips of FRP with anchored groove technique	108.5	6.1	6765	$0.41\varepsilon_{fu}$
SB2-3S-G	RC beams external strengthened with 3 Strips of FRP with anchored groove technique	132.5	6.5	7066	$0.42\varepsilon_{fu}$
SB2-4S-G	RC beams external strengthened with 4 Strips of FRP with anchored groove technique	158.5	7.0	7538	$0.45\varepsilon_{fu}$

Note: T is temperature, P_u is ultimate load, Δ_u is ultimate deflection, ε_f is CFRP strain, ε_{CFRP} is the strain in CFRP strips and ε_{fu} is the ultimate strain in CFRP strips of $16700 \mu\varepsilon$.

2. Method

2.1. Experimental Work Review

Eighteen beam specimens (2 as control, 8 strengthened with FRP with no grooves, and 8 strengthened with FRP and grooves) were built and experimented, as simply supported under four points' loading, as explicated in Fig. 1. All of the specimens were dimensioned as: 1100 mm long and 150x250 mm in cross-section. The study parameters were: the number of CFRP strips (1, 2, 3, or 4), and the existence of anchored grooves (yes, no). The mid-section of the CFRP sheets along with the both ends of the grooved specimens were anchored, perpendicularly, with 50 mm-long, 150 mm-wide grooves filled with epoxy, as illustrated in Table 1. For the ease of reference, the specimens' designations and data are listed, in brief, in Table 1; and depicted in Fig. 1.

2.2. Mix design

The concrete mixture, Table 2, consisted of the following ingredients (percentage by weight): water (0.61); Ordinary Portland cement (Type I) (1.00); Coarse aggregates (Crushed limestone) (2.98), with a maximum size of 12.5 mm, an absorption ratio of 2.3 %, and a specific gravity of 2.62; fine aggregates (2.62) with fineness modulus of 2.69, an absorption ratio of 1.9 %, and specific gravity of 2.65. To enhance the concrete mix's efficiency and produce a 50 mm-slump, a superplasticizer was added as a percent of the cement weight was.

Table 2. Design proportions for concrete mix.

Ingredient	Quantity (kg/m ³)
Water	158
Cement	269
w/c	0.40
Super- plasticizer	8
Fine aggregate	834
Coarse aggregate	891

The specimens casting procedures were as follows: to begin with, the internal surface of the 0.15 m³-in-capacity tilting drum mixer was soaked with water. Then, the coarse aggregates with some of the water were added while the mixer was turning. The next step was to add, gradually, to the mix each of the cement, water, in addition to the fine aggregates. The later step was to add the super-plasticizer with the remained

used water to the concrete mixture. Lastly, all the added components had been mixed for five minutes before was poured into molds, made of wood with inner dimensions of (150×250×1100 mm). Finally, the mixture is compacted with an electrical vibrator. Twenty-four hours post casting, the whole beams were removed from the molds, and-then-cured in lime-saturated water tank for 28 days. At age of 28 days, the cylinders' average value of the compressive strength was 25.0 MPa, while their tensile strength was 3.0 MPa.

2.3. Bonding of CFRP sheets to the concrete beams

As mentioned in the previous section, the test beams had been molded for 24 hours before they were casted and cured, for 28 days, in a lime-saturated water tank. Grooves, 5 mm wide and 50 mm long, were, then, drilled in the surfaces of the prepared beams, at the end and the middle of bonded area. Later, the drilled grooves were completely cleaned, utilizing a vacuum cleaner and a volatile liquid, aiming to get a well-dried surface for better and stronger adhesion (Fig. 2). Then, a steel wire cup brush was used to brush the to-be-bonded area, and make it rougher. This step was done to ensure having leveled contact area between the surface of the concrete and the CFRP material (Fig. 2). The dust and loose particles, resulted from the brushing, were cleaned up, using air vacuum cleaner. Then, the to-be-bonded area was marked, while the remaining area was plastered with a tape, to keep it away from epoxy (Fig. 2). For the study purposes, the CFRP sheets were cut into various lengths, with a standard width of 50 mm. The following step was to prepare the adhesive epoxy material by, slowly, mixing the two the compounds of epoxy (i.e.: part A and B) in a low-speed electric drill for at least 3 minutes, to ensure the homogeneity of the epoxy. Later, the first layer of the prepared epoxy was placed, equally, onto the marked area of bonding; and, then, the CFRP composite sheet (thickness of 0.166 mm, the tensile strength of 4900 MPa, elastic modulus of 230 GPa, and elongation at break of 2.1 %) was put on the epoxy, and was rolled over, with a plastic roller, to kick out any entrapped air bubbles. Finally, the epoxy second layer was placed on the CFRP strips so as to ensure the well epoxy distribution (Fig. 2).



Marking the area of CFRP sheets bonded using plastering tape



Drilling the grooves



Applying the first layer of epoxy onto CFRP sheets surface



Applying the two layers of epoxy onto CFRP sheets surface

Figure 2. Attachment of CFRP strips.

2.4. Testing Setup

All of the beam specimens were simply supported span of 1000 mm (Fig. 1) and experimented under four-point loading, with. The two supports included a hinge and a roller. The points of loading were a steel type to avoid deformation at ultimate load stages. A hydraulic testing machine was used to applied the load with a displacement loading rate of 0.1 mm/sec. To be able to take the values of the mid-span deflections, at the beams' bottom side, a vertical linear variable displacement transducer (LVDT) was utilized (Fig. 1). In addition, a strain gauge was installed to record the tensile strain of the CFRP material. The data

acquisition system was utilized to plot the obtained results on load-deflection curves and the CFRP strain. Whereas, the patterns of the cracking and the modes of failure were attained visually.

3. Results and Discussion

3.1. Failure Mode

Fig. 3 and 4 illustrate the modes of failure encountered by the whole beam specimens, including the control beams. The modes of failure were deliberately set to be with inclined planes, and took place inside the shear span. This was intended for the ease of evaluating the role of the CFRP strips in enhancing the concrete's shear capacity.

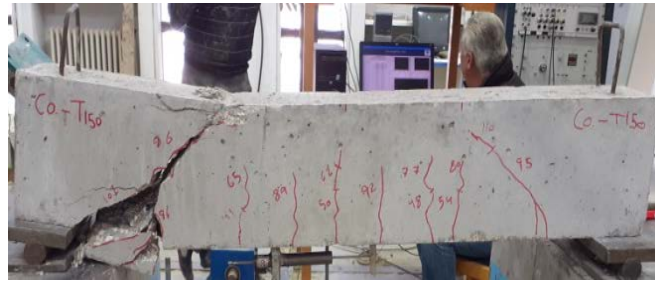
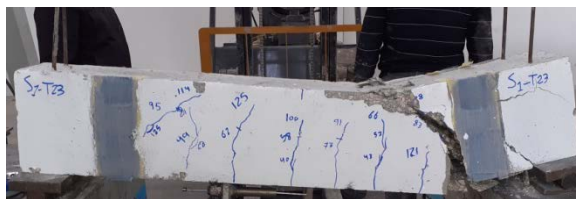


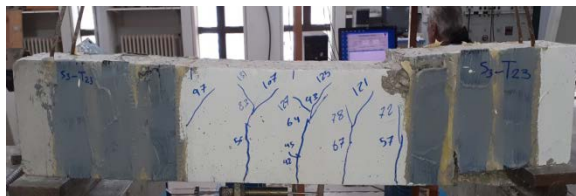
Figure 3. Typical failure mode of control beams.



(a-1) 1 CFRP strip



(a-2) 2 CFRP strips



(a-3) 3 CFRP strips



(a-4) 4 CFRP strips

(a) Without grooves



(b-1) 1 CFRP strip



(b-2) 2 CFRP strips



(b-3) 3 CFRP strips



(b-4) 4 CFRP strips

(b) With grooves

Figure 4. Typical failure mode of strengthened beams.

The emergence of web-shear cracks began through the loading process. Moreover, when the load was raised, the web-shaped cracks lengths, widths, and number increased too. When the ultimate value of loading had been reached, an enormous number of web-shaped cracks emerged, followed by an abrupt crushing inside the shear span. It had been found that the strips of CFRP had a great role in the element's resistance to shear, resulting in a variation in the ultimate values of loads, at which concrete crushing took place. When a failure occurred, a considerable amount of shear-span splintered concrete was observed, occasionally. The failure in shear, usually, happens abruptly, with a big sound, resulting in the appearance of big inclined cracks. The usual place, at which the shear failure occurs, is at either ends of the beam; that is caused by either the post-deflection loading or a very light change in the beam. It has been found that the anchored specimen's shear span had less shear cracks than the control beam; while the internal core stayed almost unharmed. The reason of this is that the utilization of the CFRP strips with anchorage system shows a great success in alleviating the developed shear stresses and cracking.

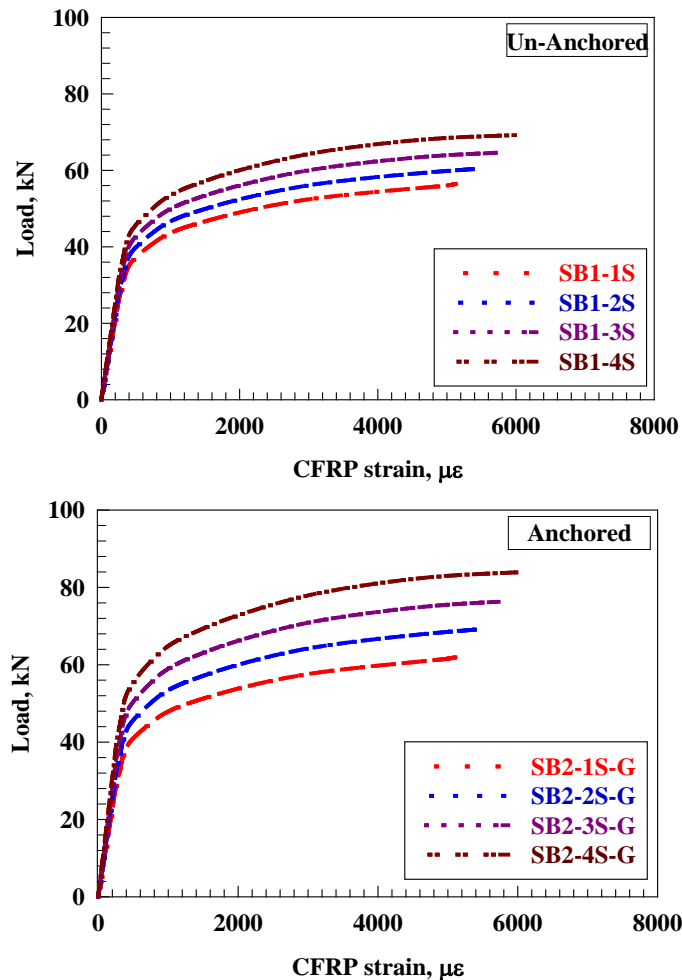


Figure 5. Typical load-CFRP strain curve.

3.2. CFRP strain

The typical curve that represents the relation between the load and the CFRP strain, for all of the tested beams, is illustrated in Fig. 5. Considering this graph, it is found that the initial appearance of in-concrete diagonal crack, resulted from the shear force, leads to developing tensile stresses in the CFRP material. In addition, it is noticed that the ultimate tensile stresses have appeared near the mid-section of the CFRP element, and crossed the diagonal cracks, close to the beam' cross-section mid-height point, as explicated in Fig. 6. It is, also, observed that all of the experimented specimens had a CFRP strain value less than 16400 $\mu\epsilon$, as illustrated in Table 1. Referring to this table, Table 1, the number of CFRP strips has, greatly, affected the efficiency of the CFRP strips, in the beams without anchoring, as follows: 31 % of the CFRP' ultimate strain when one strip was installed, 32 % when using two strips, 34 % when three strips were used, and 36 % when 4 strips. On the other side, the anchored specimens showed the following ratios: 38 % of the CFRP's ultimate strain when using one strip, 41 % when using 2 strips, 42 % when 3 strips were used, and 45 % when using 4 strips. The shown percentages indicated that the strains of the anchored beams improved by 122 % of the un-anchored ones.

The strains of the CFRP strips do not exist before the appearance of diagonal crack. When the shear strength of concrete is exceeded by the shear strength, diagonal shear cracks emerge in the shear span, while the CFRP strain keeps rising, in a rapid rate, until failure, as illustrated in Fig. 5. Also, it has been noticed that the more the area of the bonded surface, the higher the rate of the increase in the CFRP's strain. Overall, the obtained results show that grooving 4 strips of CFRP has had the best effect on the beam's behavior.

Table 3. Characteristics of load deflection behavior.

Specimen	Elastic stiffness (kN/mm)	Toughness (kN.mm ²)	SF	DF	PF	SF
SB0	12.5	139	1.00	1.00	1.00	1.00
SB1-1S	14.5	186	1.07	1.12	1.19	1.07
SB1-2S	16.5	223	1.14	1.17	1.34	1.14
SB1-3S	18.5	269	1.22	1.27	1.55	1.22
SB1-4S	20.0	301	1.31	1.30	1.71	1.31
SB2-1S-G	16.0	230	1.17	1.22	1.44	1.17
SB2-2S-G	20.0	282	1.31	1.28	1.67	1.31
SB2-3S-G	24.0	347	1.44	1.37	1.97	1.44
SB2-4S-G	27.5	433	1.59	1.48	2.35	1.59

Note: SF is strength factor, DF is ductility factor, PF is performance factor = SFxDF, STF is stiffness factor

3.3. Load-deflection behavior

Table 3 illustrates the load vs. the mid-span deflection responses and the characteristics (stiffness and roughness) of the three groups of the specimens, i.e.: the un-anchored, the anchored, and the control. The initial stiffness ($k = P/\delta$) is demarcated as "the slope of linear elastic portion of load-deflection response"; whereas the toughness is defined as "the area underneath the load-deflection response until ultimate load capacity". The load-deflection curves, Fig. 6 have three sections: a) the linear section, from the starting point till the emergence of the first flexural crack; b) the transitional section, extends from the end of the previous section till the emergence of the diagonal shear crack; and c) the after-cracking section, up to ultimate beam capacity. Fig. 6 and Table 3 show, explicitly, that the anchoring method has impacted the load-deflection characteristics curve, in terms of: ultimate deflection, ultimate load, stiffness, and toughness. In addition, it has been found that the anchored specimens performed better with the increase in the CFRP bonded area.

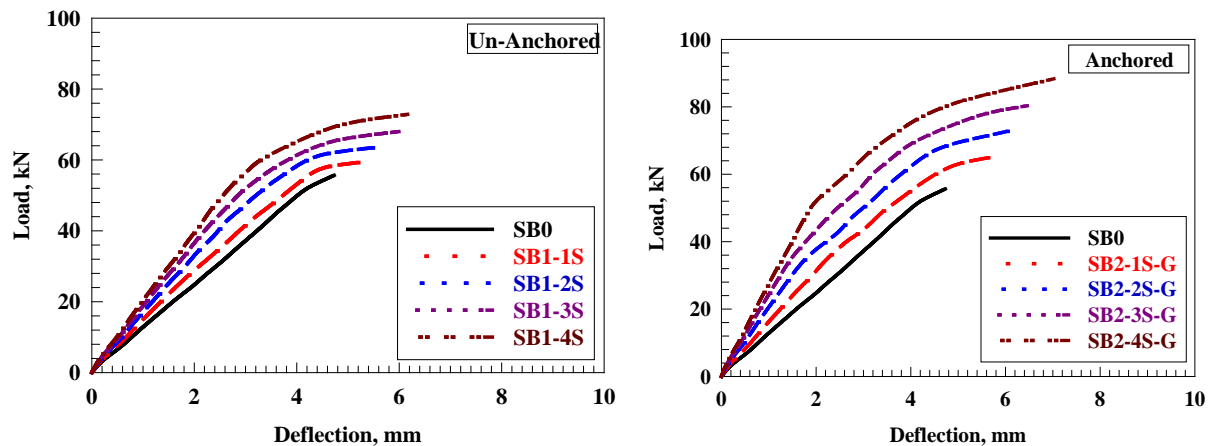


Figure 6. Load-deflection curves for the tested beam.

3.4. Ultimate load capacity and corresponding deflection

Upon evaluating the specimens' load capacity and the resulting deflection, it has been found that the structures performed very well. In the reinforced members, the deflection is associated with the structural serviceability; where the ultimate load capacity can be connected to ultimate load limit states, as seen in Table 3. The percentages of the load capacity are determined by dividing the ultimate load capacity of the strengthened beam by the ultimate load capacity of the control beam; while the deflection can have determined by dividing the strengthened beam's ultimate deflection by the load capacity of the control beam, as explicated in Fig. 7. The term (deflection) is an indicator of the reinforced beam's capability of enduring deformations, without the occurrence of failure. The deflection percentage can be specified by

dividing the strengthened beam's ultimate deflection by the ultimate deflection of the control beam (undamaged beam), as explicated in Fig. 8.

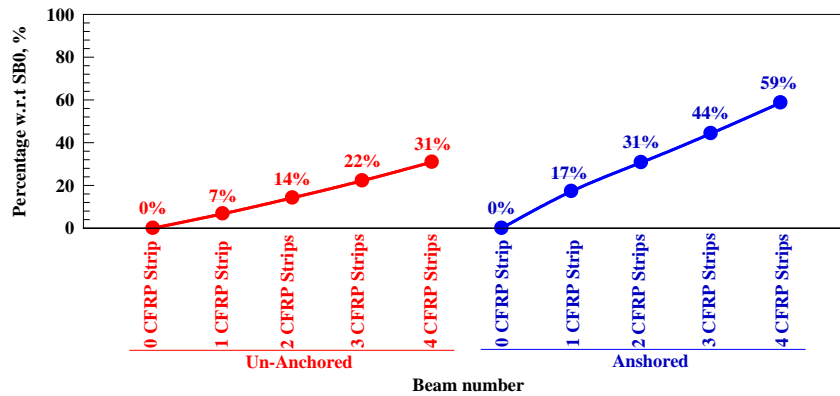


Figure 7. Ultimate load capacity enhancement percentage with respect to control beam.

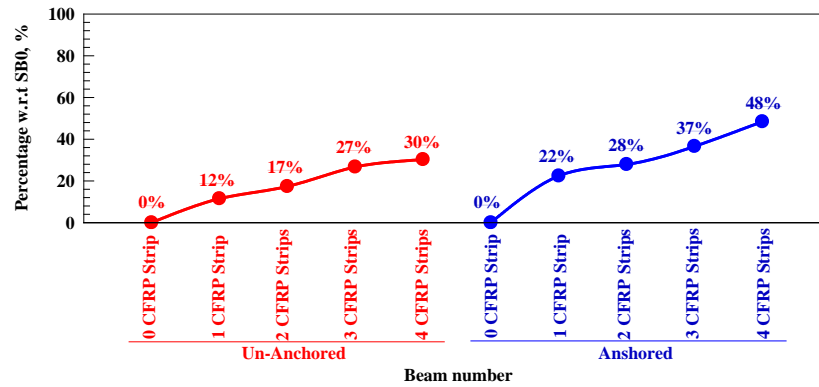


Figure 8. Ultimate deflection enhancement percentage with respect to control beam.

3.5. Elastic stiffness

The elastic stiffness determines the crystal's response when exposed to external forces, e.g.: stress or strain. Also, it is a clear indicator of the bonding's quality and stability, mechanically and structurally. In the load vs. deflection curve, the elastic stiffness is represented by the slope of the pre-cracking section. For the ease of comparison, every strengthened-beam's elastic stiffness was normalized with respect to the un-strengthened control beam, as illustrated in Fig. 9. It has been found that the more the CFRP strips, the higher the percentage of the elastic stiffness. The percentages of the un-anchored beams' elastic stiffness (Fig. 10) are: 17 % when 1 strip of CFRP is used, 33 % for 2 strips, 47 % for 3 strips, and 59 % for 4 strips; showing an enhancement average of 39 %. As for the reinforced beams with anchorage, the ratios of the elastic stiffness (Fig. 9) have reached to: 26 % upon using 1 strip of CFRP, 61 % when 2 strips, 91 % with 3 strips, and 117 % with 4 strips, with an enhancement average of 74 %. The enhancement in the anchored beams' stiffness is 1.90 times better than those without anchoring.

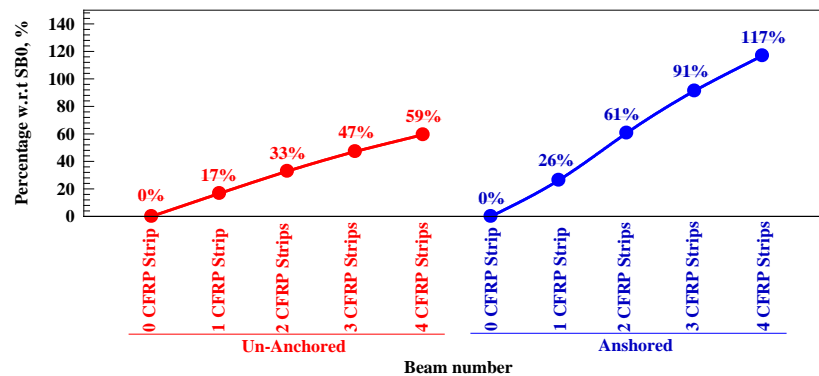


Figure 9. Stiffness enhancement percentage with respect to control beam.

3.6. Toughness

Toughness indicates the material's capability of absorbing energy and deforming, plastically, without being broken. It can be defined as the material's energy absorption (per unit volume) before breaking down. Toughness can be mathematically found by calculating the total area beneath the load vs. deflection curve.

It must be noticed that each strengthened-by-CFRP beam's toughness has been normalized with respect to the control beams, as explicated in Fig. 10. It has been shown in Fig. 10 that increasing the strips of CFRP results in raising the beam's toughness, considerably. For the beams with no anchoring, the toughness (Fig. 10) has reached to: 34 % when using 1 CFRP strip, 61 % when 2 strips are used, 94 % when using 3 strips, and 117% when using 4 strips, with an enhancement of 77 %. As for the beams with anchorage, the percentages of toughness (Fig. 10) has reached to: 66 % when using 1 strip of CFRP, 103 % when using 2 strips, 150 % when using 3 strips, and 212 % when using 4 strips, with an enhancement of 133 %. This result shows that toughness percentage of the anchored specimens is 1.73 times more than the un-anchored ones.

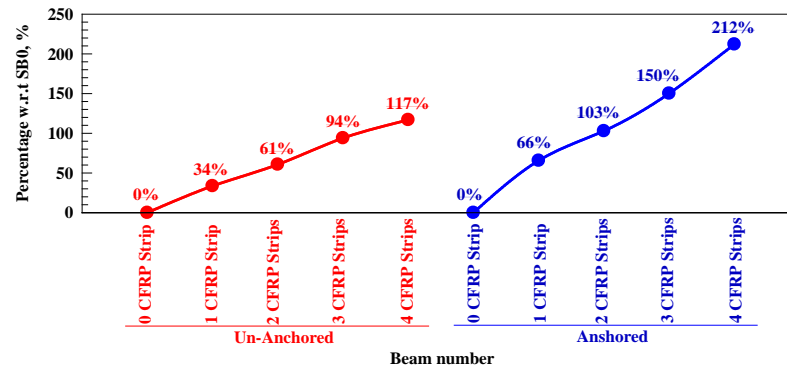


Figure 10. Toughness enhancement percentage with respect to control beam.

3.7. Performance of Tested Beams

To explore the impact of the CFRP material on the reinforced RC beams, the following factors have been evaluated: the strength factor (SF), the deformability factor (DF), and the performance factor (PF), making sure that the beams are normalized with respect to the control beams. All of the factors act together to for the total performance of a structure, as illustrated in Fig. 11. As it is explicated in Fig. 11, increasing the area of bonding, results in raising the whole factors (DF, SF, and PF). Further, raising the area of bonding results in a significant improvement in the beam's performance, close to control beams, and prevented brittle shear failure. The anchored strengthened-with-CFRP beams exhibited much better performance than the un-anchored ones. Thus, it can be concluded that utilizing the CFRP sheets to reinforcing the beams has proven to be much more effective and showed remarkable results than the CFRP strips on the web.

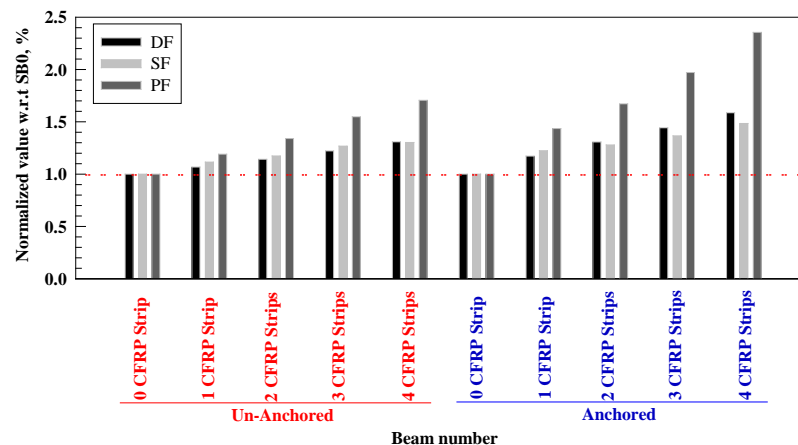


Figure 11. Normalized performance characteristic factors.

3.8. Profitability Index of the Number of CFRP Strips

Table 5 demonstrates: the concrete shear strength (V_c), CFRP shear strength (V_f), and the ultimate load capacity, obtained from experimenting RC beam specimens, that were reinforced with different methods- using CFRP composites. In addition, Table 4 shows that adding more strips of CFRP or enlarging the bonding surface has resulted in an increase in the (V_f). The indices of profitability had to be calculated to be able to assess the effectiveness of several methods of reinforcement using CFRP materials, regarding the consumed quantity of CFRP. It must be mentioned that the profitability index expresses the ratio of CFRP contribution in shear within the shear span to the total CFRP bonded area. Table 4 demonstrates the values of the profitability indices, for a number of reinforcing techniques. From Table 4, it is shown that

the un-anchored beams have a profitability index of (in MPa): 1.15 when using 1 strip of CFRP, 1.10 when using 2 strips, 1.05 for 3 strips, and 1.00 for 4 strips. On the other side, the anchored beams have the following values of profitability index (in MPa): 2.56 using 1 strip of CFRP, 2.28 using 2 strips, 2.19 using 3 strips, and 2.18 using 4 strips. This shows that the anchored beams' index of profitability is 2.2 times more than the un-anchored ones.

Table 4. Profitability index of CFRP strips.

Beam number	V_c , kN	V_f , kN	V_u , kN	V_f/A_f , MPa
SB0	55.7	0.0	55.7	---
SB1-1S	55.7	3.8	59.4	1.15
SB1-2S	55.7	7.9	63.6	1.10
SB1-3S	55.7	12.4	68.0	1.05
SB1-4S	55.7	17.2	72.9	1.00
SB2-1S-G	55.7	9.6	65.3	2.56
SB2-2S-G	55.7	17.1	72.8	2.28
SB2-3S-G	55.7	24.7	80.3	2.19
SB2-4S-G	55.7	32.7	88.3	2.18

Note: V_c is the concrete shear strength, V_f is the CFRP shear strength, A_f is the total CFRP bonded area

3.9. Comparison of experimental results with the ACI model

or the sake of comparison, the obtained results have been compared with ACI model [1]. The guidance for the general design was attained from the experimental data, and they were solely valid for the external FRP reinforcement. Fig. 12 depicts the predicted values of the ACI model ($V_{f, experimental}/V_{f, ACI}$ [1]), and a comparison among them. It must be noted that the ACI model is adjusted to use for CFRP; therefore, extreme caution must be taken when using this model for other composites, as illustrated in Fig. 12. The overall ACI model's [1] predictions have been overvalued, with a mean $V_{f, experimental}/V_{f, ACI}$ value of 1.11 and a coefficient of variation (COV) of 26 %. It must be noted, also, that the obtained values, from the ACI model, are overrated, and based on the values of parameters extracted from the experimental data of the strengthened-by-FRP-laminates beams. However, the ACI model is not valid for all case. Further, the ACI model has a, vastly, broad range of experimental/theoretical failure load ratios from 0.80 to 1.46, as explicated in Fig. 12.

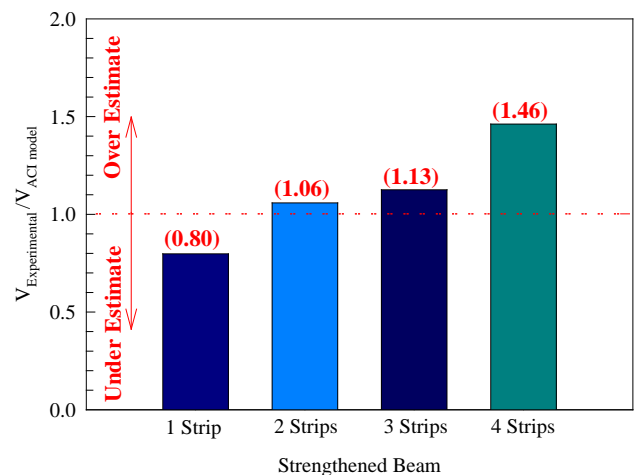


Figure 12. The ratio of experimental FRP shear force to calculated one using ACI model [1].

4. Conclusions

1. The ill-timed de-bonding issue is frequently encountered by the unanchored strengthened-by-FRP beams; unlike the anchored ones, which have a less serious failure mode, which is concrete cover separation.

2. The technique of the anchored grooves converted the dangerous modes of failure, i.e.: separation of concrete cover or in-between-surfaces de-bonding, to a less serious mode. This has enhanced the performance quality of the traditional techniques of FRP-reinforcement.

3. The method of anchored grooves has proven a great efficiency in strengthening RC beams because it enlarges the shear capacity of the anchorage region.

4. The anchored grooves method enhanced the RC beams' capacity of load-carrying, and minimized, considerably, the mid-span vertical deflection, compared with the control un-strengthened beam.

5. In contrast to the control beams, the anchored grooves method enhanced the RC beams': ultimate load capacity, stiffness, toughness; while it reduced the deflections. Also, this method availed an improved structural performance factor.

6. All of the predictions of the ACI model [1] have been overrated, where the mean value reaching 1.11, and the coefficient of variation (COV) of 26 %.

References

1. ACI Committee 440. Design and Construction of Externally Bonded FRP Systems for strengthening Concrete Structures. *ACI440.2R-02. 2002. American Concrete Institute, Farmington Hills, Mich.: 45 pp. DOI: 10.1061/40753(171)159. ISBN: 9780870312854
2. Wenwei, W., Guo, L. Experimental study and analysis of RC beams strengthened with CFRP laminates under sustained load. *International Journal of Solids and Structures*. 2006. 43(1). Pp. 1372–1387. DOI: 10.1016/j.ijsolstr.2005.03.076
3. Aram, M.R., Czaderski, C., Motavalli, M. Debonding failure modes of flexural FRP-strengthened RC beams. *Composites: Part B*. 2008. 39(1). Pp. 826–841. DOI: 10.1016/j.compositesb.2007.10.006
4. Thomsen, H., Spacone, E., Limkatanyu, S., Camata, G. Failure Mode Analyses of Reinforced Concrete Beams Strengthened in Flexure with Externally Bonded Fiber-Reinforced Polymers. *Journal of Structural Engineering-ASCE*. 2004. 2(123). Pp. 1090–0268. DOI: 10.1061/(ASCE)1090-0268(2004)8:2(123)
5. El-Ghandour A. Experimental and analytical investigation of CFRP flexural and shear strengthening efficiencies of RC beams. *Construction and Building Materials*. 2011. 25(1). Pp. 1419–1429. DOI: 10.1016/j.conbuildmat.2010.09.001
6. Rajai, Z. Al-Rousan, Mohammad, F. AL-Tahat. Consequence of surface preparation techniques on the bond behavior between concrete and CFRP composites. *Construction and Building Materials*. 2019. 212(1). Pp. 362–374. DOI: 10.1016/j.conbuildmat.2019.03.299
7. Pham, H., Al-Mahaidi, R. Experimental investigation into flexural retrofitting of reinforced concrete bridge beams using FRP composites. *Composite Structures*. 2004. 66(1). Pp. 617–625. DOI: 10.1016/j.compstruct.2004.05.010
8. Al-Rousan, R. Behavior of CFRP Strengthened Columns Damaged by Thermal Shock. *Magazine of Civil Engineering*. 2020. 5(97). Pp. 90–100. DOI: 10.18720/MCE.97.5
9. Al-Rousan, R. Behavior of strengthened concrete beams damaged by thermal shock. *Magazine of Civil Engineering*. 2020. 94(2). Pp. 93–107. DOI: 10.18720/MCE.94.2
10. Travush, V.I., Konin, D.V., Krylov, A.S. Strength of reinforced concrete beams of high-performance concrete and fiber reinforced concrete. *Magazine of Civil Engineering*. 2018. No. 77(1). Pp. 90–100. DOI: 10.18720/MCE.77.8
11. Al-Rousan, R., Abo-Msamh, Isra'a. Bending and Torsion Behaviour of CFRP Strengthened RC Beams. *Magazine of Civil Engineering*. 2019. 92(8). Pp. 62–71. DOI: 10.18720/MCE.92.8
12. Mohammad, A. Alhassan, Rajai, Z. Al-Rousan, Ahmad M. Abu-Elhija. Anchoring holes configured to enhance the bond-slip behavior between CFRP composites and concrete. *Construction and Building Materials*. 2020. 250(1). Pp. 118905. DOI: 10.1016/j.conbuildmat.2020.118905
13. Ayman, S. Mosallam, Swagata Banerjee. Shear enhancement of reinforced concrete beams strengthened with FRP composite laminates. *Composites Part B Engineering*. 2007. 38(5-6). Pp. 781–793. DOI: 10.1016/j.compositesb.2006.10.002
14. Anil, O., Belgin, C.M. Anchorages effects on CFRP-to-concrete bond Strength. *Journal of Reinforced Plastic and Composites*. 2010. 29(1). Pp. 539–557. DOI: 10.1177/0731684408100259
15. Diab, H., Wub, Z., Iwashita, K. Short and long-term bond performance of prestressed FRP sheet anchorages. *Engineering Structures*. 2009. 31(1). Pp. 1241–1249. DOI: 10.1016/j.engstruct.2009.01.021
16. Smith, S.T., Hua, S., Kim, S.J., Seracino, R. FRP-strengthened RC slabs anchored with FRP anchors. *Engineering Structures*. 2011. 33(1). Pp. 1075–1087. DOI: 10.1016/j.engstruct.2010.11.018
17. El Maaddawy, T., Soudki, K. Strengthening of reinforced concrete slabs with mechanically-anchored unbonded FRP system. *Construction and Building Materials*. 2008. 22(1). Pp. 444–455. DOI: 10.1016/j.conbuildmat.2007.07.022
18. Ceroni, F., Pecce, M., Matthys, S., Taerwe, L. Debonding strength and anchorage devices for reinforced concrete elements strengthened with FRP sheets. *Composites: Part B*. 2008. 39(1). Pp. 429–441. DOI: 10.1016/j.compositesb.2007.05.002
19. Bank, L., Arora, D. Analysis of RC beams strengthened with mechanically fastened FRP (MF-FRP) strips. *Composite Structures*. 2007. 79(1). Pp. 180–191. DOI: 10.1016/j.compstruct.2005.12.001
20. Al-Mahmoud, F., Castel, A., François, R., Tourneur, C. Anchorage and tension-stiffening effect between near-surface-mounted CFRP rods and concrete. *Cement and Concrete Composites*. 2011. 33(1). Pp. 346–352. DOI: 10.1016/j.cemconcomp.2010.10.016
21. Kalfat, R., Al-Mahaidi, R., Smith, S.T. Anchorage Devices used to improve the Performance of Reinforced Concrete Beams Retrofitted with FRP Composites: A-State-of-the-Art-Review. *Journal of Composites for Construction*. 2013. 17(1). Pp. 14–33. DOI: 10.1061/(ASCE)CC.1943-5614.0000276
22. Hugo, C. Biscaia, Rui Micaelo, João Teixeira, Carlos Chastre. Numerical analysis of FRP anchorage zones with variable width. *Composites Part B: Engineering*. 2014. 67(1). Pp. 410–426. DOI: 10.1016/j.compositesb.2014.07.031
23. Lamanna, A.J., Bank, L.C., Scott, D.W. Flexural Strengthening of Reinforced Concrete Beams Using Fasteners and Fiber-Reinforced Polymer Strips. *ACI Structural Journal*. 2001. 98(3). Pp. 368–676. DOI: 10.14359/10225
24. Spadea, G., Bencardino, F., Swamy, R.N. Structural behavior of composite RC beams with externally bonded CFRP. *Journal of Composite Construction*. 1998. 2(3). Pp.132–137. DOI: 10.1061/(ASCE)1090-0268(1998)2:3(132)

25. Lam, L., Teng, J.G. Strength of RC cantilever slabs bonded with GFRP strips. *Journal of Composite Construction*. 2001. 5(4). Pp. 221–227. DOI: 10.1061/(ASCE)1090-0268(2001)5:4(221)
26. Micelli, F., Rizzo, A., Galati, D. Anchorage of composite laminates in RC flexural beams. *Structural Concrete*. 2010. 11(3). Pp. 117–126. DOI: 10.1680/stco.2010.11.3.117
27. Wu, Y.F., Huang, Y. Hybrid bonding of FRP to reinforced concrete structures. *Journal of Composite Construction*. 2008. 12(3). Pp. 266–273. DOI: 10.1061/(ASCE)1090-0268(2008)12:3(266)
28. Biscaia, H.C., Chastre, C. Design method and verification of steel plate anchorages for FRP-to-concrete bonded interfaces. *Composite Structures*. 2018. 192(1). Pp. 52–66. DOI: 10.1016/j.compstruct.2018.02.062
29. Pellegrino, C., Modena, C. Flexural Strengthening of Real-Scale RC and PRC Beams with End-Anchored Pretensioned FRP Laminates. *ACI Structural Journal*. 2009. 106(3). Pp. 319–328. DOI: 10.14359/56496
30. Biscaia, H.C., Chastre, C., Cruz, D., Franco, N. Flexural Strengthening of Old Timber Floors with Laminated Carbon Fiber-Reinforced Polymers. *Journal of Composites for Construction*. 2019. 21(1). Pp. 04016073. DOI: 10.1061/(ASCE)CC.1943-5614.0000731

Information about authors:

Rajai Al-Rousan, PhD

ORCID: <https://orcid.org/0000-0001-6981-7420>

E-mail: rzalrousan@just.edu.jo

Received 09.10.2020. Approved after reviewing 06.04.2021. Accepted 06.04.2021.